Indian Journal of Pure & Applied Physics
Vol. 61, July 2023, pp. 554-559
DOI: 10.56042/ijpap.v61i7.101

Simulation of Optical Characteristics of a Breast Tumor Incorporated with Silica Coated Gold Nanorods

Vikas[a,b], Rizul Gautam[a,b] & Sanjeev Soni[a,b]*

[a]Biomedical Applications Group, CSIR - Central Scientific Instruments Organisation, Sector-30C, Chandigarh 160 030, India
[b]Academy of Scientific and Innovative Research (AcSIR), Ghaziabad 201 002, India

Received 15 October 2022; accepted 12 June 2023

Silica coated nanoparticles are advantageous in terms of enhanced biocompatibility, colloidal and thermal stability as well as ease of surface functionalization for use in various biomedical applications. Specifically, for plasmonic photothermal therapeutics and photothermally modulated drug delivery, it is always desired to have maximum absorption of the incident EM radiation by the nanoparticles. So, it is required to quantify the absorption cross-section (σ_{abs}) of silica coated gold nanorods (GNRs) of varying silica coating thickness. Here, the optical properties of silica coated GNRs embeded in breast tumor like medium are computed for 10×41 nm GNRs which are considered to be coated (dense) with silica thickness range of 1-20 nm. Also, periodic and random spatial distributions of these GNRs within the tumor are accounted for calculating the effect of silica thickness on the overall optical properties. For this, finite element method is used wherein the propagation of incident elecromagnetic field is assumed to be perpendicular to the longitudinal axis of GNRs. Results show that for GNRs coated with silica thickness of 1 nm, the plasmonic wavelength is red-shifted by 40 nm as compared to bare GNRs. Furthermore, on increasing the silica thickness from 2-20 nm, plasmonic wavelength is red-shifted by 24 nm.The absorption and scattering cross-section are increased by ~4.5% and ~8% for GNR coated with 1 nm silica as compared to the bare GNR. Further, it is seen that the scattering cross-section of the media is significantly enhanced by ~26% with an increase in silica thickness from 1-20 nm, while there is no significant change in absorption cross-section for higher silica coating thickness up to 20 nm. Considering the spatial distribution of GNRs within the tumor, the σ_{abs} values is increased by ~44% for periodically distributed silica coated GNRs as compared to random distribution within the tumor domain. Also, it is observed that the electric field is confined close to the Gold-Silica interface for lower thickness of the silica coating. These discussed results are useful for the selection of silica coating thickness on GNRs for the biomedical applications such as plasmonic photothermal therapy and photothermally modulated drug delivery.

Keywords: Silica coating; Gold nanorods; Plasmonic photothermal; Optical absorption cross-section

1 Introduction

Silica coated metallic nanoparticles are of potential use in biomedical applications such as cancer imaging, diagnosis, therapeutics, drug delivery, *etc*.[1-4]. Gold nanorods coated with silica (GNRs@SiO_2) are biocompatible with high colloidal and thermal stability and show high photothermal conversion efficiency during the interaction of light and nanoparticles[5-7]. The temperature rise of gold nanorods (GNRs) suspension during the interaction with incident electromagnetic field is largely affected due to the variation in shape, size, refractive index of medium, and wavelength of incident beam[8,9]. The optical characteristics such as absorption and scattering cross-section, and plasmonic wavelength of gold nanorods embedded medium play an important role to identify the heat generation in the medium during plasmonic photothermal therapy[10,11]. For silica coated nanorods, the optical characteristics of GNRs@SiO_2 are highly affected due to the change in thickness of the silica layer as well as the porosity of silica coating[12]. It is required to estimate the role of silica thickness on the optical characteristics of GNRs@SiO_2 embedded tumor to choose a suitable coating thickness of GNRs@SiO_2 based on the parameters of incident beam for plasmonic photothermal therapy. In literature, the experimental measurement of the absorbance for various silica thickness has been reported[12]. It is reported that the absorbance peak of the suspension is red-shifted with an increase in the thickness of silica coating. There is a need to quantify the effect of silica coating thickness on the optical properties of a tumor immerse with GNRs@SiO_2. Further, the effect of periodic and random spatial distribution of GNRs@SiO_2 on the optical properties of tumor needs to be addressed.

*Corresponding author: (E-mail: ssoni@csio.res.in)

Here, the optical properties such as absorption and scattering cross-section, and plasmonic wavelength of a breast tumor embedded with GNRs@SiO_2 are computed by considering the silica coating thickness range of 1-20 nm. Further, the optical properties are computed by considering the spatial distribution of GNRs@SiO_2 within the tumor medium. The discussed results are useful for various biomedical applications involving use of GNRs@SiO_2.

2 Theory and methods

Here, the electric field distribution and spectral variation in optical properties of silica coated GNRs is computed by using the finite element method[11,13]. In this study, the FEM model is implemented using a wave optics module in COMSOL Multiphysics. The electric field distribution inside the medium is evaluated by using Helmholtz approximation as per Eq. 1[18],

$$\nabla \times \left(\mu_r^{-1}\nabla \times \vec{E}\right) - k_0^2\left(\varepsilon_r - j\frac{\tau}{\omega\varepsilon_0}\right)\vec{E} = 0 \quad (1)$$

where k_0, μ_0, σ, ε_0, and ε_r are wave number, the relative permeability of medium, conductivity, vacuum permittivity, and relative permittivity of medium respectively[11]. During the evaluation of electric field distribution, the dielectric permittivity of GNRs is considered for a spectral range of 600 nm to 1000 nm defined as[14,18],

$$\varepsilon_r(\omega) = \varepsilon_\infty + \sum_{j=1}^{M}\frac{f_j\,\omega_P^2}{\omega_{0j}^2 - \omega^2 + i\gamma\omega} \quad (2)$$

Here, γ is damping coefficient, ω_{0j} is resonance frequency, ω_P is plasma frequency, ε_∞ is relative permittivity, and f_j is oscillator strength respectively[11]. As shown in equation 3, the absorption cross-section ($\boldsymbol{\sigma_{abs}}$) of silica coated GNRs is calculated by volumetric integration of absorbed power over nanoparticle volume (V) per unit of incident power[11,13,18].

$$\sigma_{abs} = \frac{1}{I_{inc}}\iiint Q_{loss}\, dV \quad (3)$$

The total absorbed power can be used to compute the power loss density Q_{loss} (W/cm^2) due to the incident field's absorption[18].

Further, the scattering cross-section ($\boldsymbol{\sigma_{sca}}$) of GNRs in the medium is calculated by boundary integration of scattered power over the surface of particles w.r.t incident power as[13],

$$\sigma_{sca} = \frac{1}{I_{inc}}\iint (\vartheta . P_{sca})\, dV \quad (4)$$

Here, P_{sca} (units of W/m^2) is the time-average of the Poynting vector and ϑ normal pointing vector outwards from the particle.

For solving the Helmholz wave equation, the polarization of incident field is considered parallel to longitudinal axis of GNR and direction of the incident electric field is considered perpendicular to longitudinalaxis of GNRs[11].

In this study, tumor medium embedded with 10×41 nm GNRs, which posses maximum absorption of incident electromagnetic energy within the therapeutic window of biological tissue[15,16]. During computation, the silica coated GNRs of concentration 20 µg/ml and 200 µg/ml in breast tumor of refractive index 1.40 are considered[17,18]. The 20 µg/ml concentration of silica coated GNRs is selected based on our earlier experimental study, wherein we found this concentration of GNRs can raise the temperature of a medium up to ~14 °C[22]. To evaluate optical properties of the medium embedded with GNRs@SiO_2 of concentration 200 µg/ml in breast tumor, a domain of diameter 1200 nm is considered. The geometric and computational domains for random spatial distribution are shown in Fig. 1(a) and 1(b) respectively. For this study, GNRs@SiO_2 are located within the center of the domain.

The domain's outer layeris considered as an optically perfect matched layer (PML) to reduce the impact of scattered light through the domain's boundary[11,18]. While the distribution of scattered light through particles inside the medium is evaluated by considering the inner surface of PML as a perfect electric conductor[18]. The tumor domain is tetrahedrally meshed with fine meshing[18]. The elements size of GNRs@SiO_2 ranges from 1.4-11.2 nm, and of tumor domain 3-100 nm, and there are total about ~1×10^6 elements as shown in Fig. 1(b). The optical characteristics were evaluated by solving the electromagnetic field distribution inside the domain using the biconjugate gradient stabilized method (BiCGStab). The uniform silica coating on GNR of various thickness was considered for this study.

3 Results and discussion

The computed results from the numerical model, for estimation of absorption and scattering cross-section, are verified by comparing the σ_{abs} of bare GNR with the literature reported values[18,19]. The

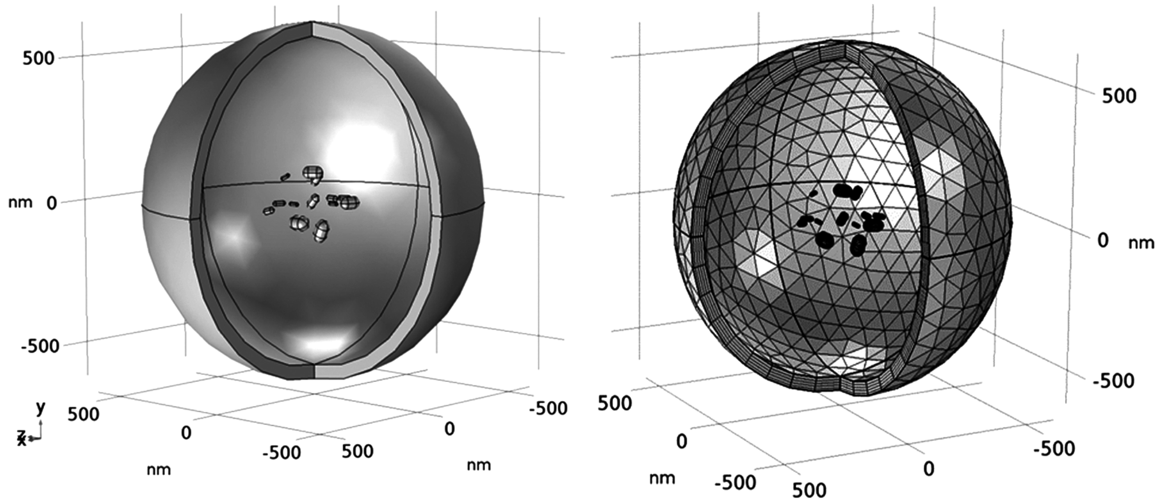

Fig. 1 — (a) Geometrical, and (b) meshed model of breast tumor domain (refractive index 1.40) embedded with $GNRs@SiO_2$ of diameter 10 nm and length 41 nm of concentration 200 µg/ml. The particles with various silica coating thickness are randomly distributed in the medium.

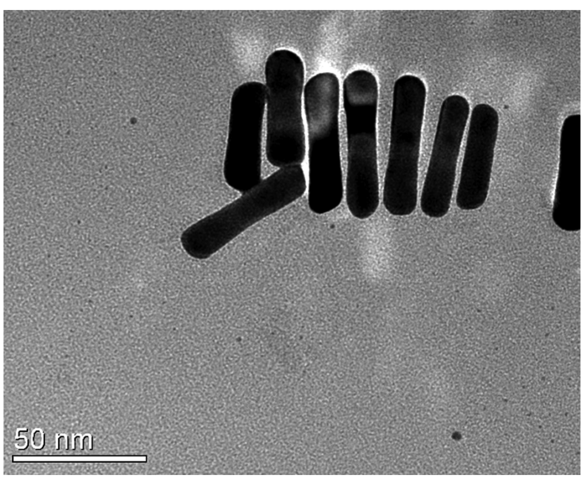

Fig. 2 — Transmission electron microscopy image of the synthesized GNRs.

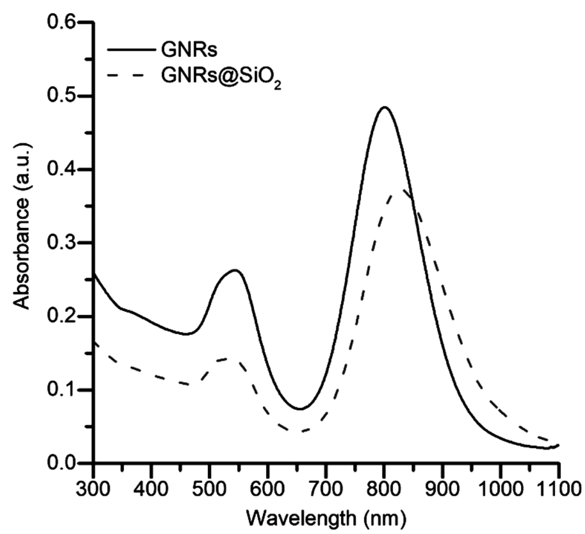

Fig. 3 — Measured spectral absorbance of GNRs and $GNRs@SiO_2$.

reported (FDTD model) and computed (FEM model) result shows, that the σ_{abs} of GNR of diameter 9 nm and aspect ratio 3.8 in the water domain is 2450 nm^2 (reported) and 2660 nm^2 (computed) respectively[11]. So, a significant matching between computed and reported values of σ_{abs} is observed.

3.1 Characterisation of GNRs and $GNRs@SiO_2$

Here, the bare GNRs with an aspect ratio of ~4.1 were prepared by using seed mediated method, and silica coated gold nanorods were synthesized using the protocol reported by Nikoobhat[20,21]. To examine the synthesized gold nanorods in terms of shape and size, TEM (transmission electron microscopy) analysis was performed. Fig. 2 revealed that the synthesized nanomaterial is in the shape of nanorods with an average length of ~41 nm and width of ~ 10 nm respectively.

The absorbance spectrum of bare GNRs and silica coated GNRs measured by using a UV-VIS spectrophotometer (UV-3200, Labindia Instruments Pvt. Ltd.) are shown in Fig. 3. From Fig. 3, it is seen that the absorbance spectra of GNRs and $GNRs@SiO_2$ shows two distinct peak corresponding to transverse and longitudinal surface plasmon resonance. On comparing both spectra, a red shift in longitudinal surface plasmon resonance (LSPR) peak due to the silica coating from 803 nm to 827 nm was observed. This red shifting of peak can be due to a change in the refractive index of surrounding medium as in the case of GNRs refractive index of surrounding media is 1.33 and in case of GNRs@SiO_2, refractive index is 1.46.

3.2 Silica coating thickness dependent optical characteristics of breast tumor in presence of GNRs@SiO_2

The values of σ_{abs} and σ_{sca} of breast tumor embedded with silica coated gold nanorods (GNRs@SiO_2) of concentration 20 µg/ml are shown in Fig.s 4(a) and 4(b) respectively. Further, the thickness dependent variation in the plasmonic wavelength of tumor media embedded with GNRs@SiO_2 is shown in Fig. 4(c). Here, the entire computational domain is considered as dielectric media (tumor) of refractive index 1.40[17].

From Fig. 4(a), it is observed that the values of σ_{abs} of silica coated GNR for a silica thickness of 1 nm increases by ~4.5% as compared to bare GNR. Further, it is observed that the peak σ_{abs} of GNRs@SiO_2 increases slightly with an increase in the silica thickness from 1-20 nm. Fig. 4(b) shows the scattering cross-section of breast tumors embedded with GNRs@SiO_2 of varying thickness. The σ_{sca} of breast tumor media embedded with silica coated GNR of thickness 1 nm enhances the scattering by ~8% as compared to bare GNR. Further, from Fig. 4(b) it is observed that due to an increase in thickness of silica coating 1-20 nm on GNR, the scattering cross-section of media was significantly enhanced by ~26%. From Fig. 4(c), it is observed that the plasmonic wavelength of media is red-shifted by 24 nm (852 nm to 876 nm) on increasing the silica thickness from 1 nm to 20 nm. The computed results of the silica thickness dependent variation in the plasmonic wavelength of GNRs@SiO_2 shows a similar trend to the experimental results. Due to the change in the surrounding medium, the computed results show a higher shift in plasmonic wavelength as compared to measured spectral absorbance (Fig. 3).

By comparing the experimental values with the computed results, it is found that the experimental values of absorption cross section for 10×41 nm^2 bare GNR in water is 7490 nm^2, which is a bit lower than the computed absorption cross section of 9200 nm^2 [23]. Overall, the silica coating on GNRs not only enhances the absorption and scattering cross-section of the media but also shows a red-shift in plasmonic wavelength of GNRs@SiO_2 as seen in Fig. 4. The electric field distribution of silica coated GNR on interaction with incident field for silica coating thicknesses of 1 nm, 3 nm, 5 nm, and 10 nm are shown in Fig. 5 respectively.

From Fig. 5, it is inferred that the normalized amplitude of the electric field achieved by GNRs@SiO_2 inside the medium is equal for silica coating thicknesses of 1-10 nm respectively. Further, it is observed that for silica thickness up to 5 nm, the electric field is prominent up to the surface of silica coating, while for silica thickness >5 nm, the field is confined within the core of silica coating.

3.3 Effect of the spatial distribution of GNRs@SiO_2 within the tumor

The spectral variation in the σ_{abs} of breast tumor in presence of GNRs@SiO_2 of random silica coating of thicknesses 1-20 nm & concentration 200 µg/ml are shown in Fig.s 6(a) and 6(b). During this study, the 10×41 nm GNRs coated with different thicknesses of silica were considered to be incorporated in breast tumor with periodic and random spatial arrangements respectively.

Figure 6(a) shows the spectral variation in absorption cross-section of breast tumor embedded with GNRs@SiO_2 of silica thicknesses 1 nm, 5 nm, and 10 nm with periodic and random spatial distributions within the domain. From Fig. 6(a), it is seen that the peak σ_{abs} for the periodic spatial

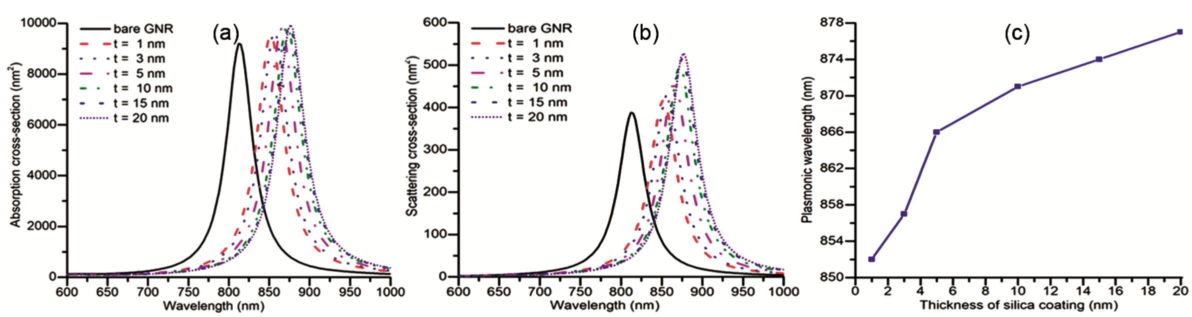

Fig. 4 — Spectral variation in (a) absorption and (b) scattering cross-sections of bare GNR and GNRs@SiO_2 in breast tumor (refractive index 1.40) for silica thickness of 1-20 nm, and (c) thickness dependent shift in plasmonic wavelength of breast tumor embedded with GNRs@SiO_2.

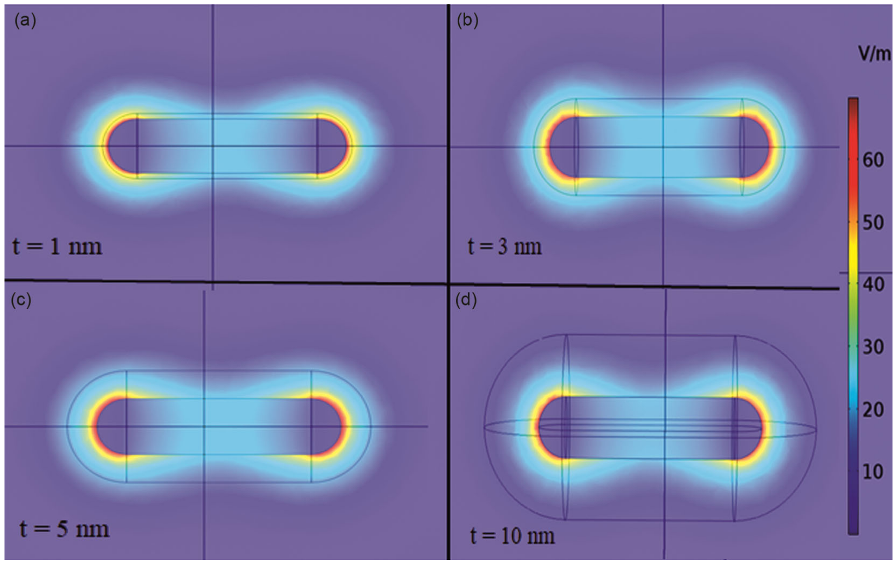

Fig. 5 — Electric field distribution of GNRs@SiO_2 for silica thicknesses of 1 nm, 3 nm, 5 nm, and 10 nm at plasmonic wavelength.

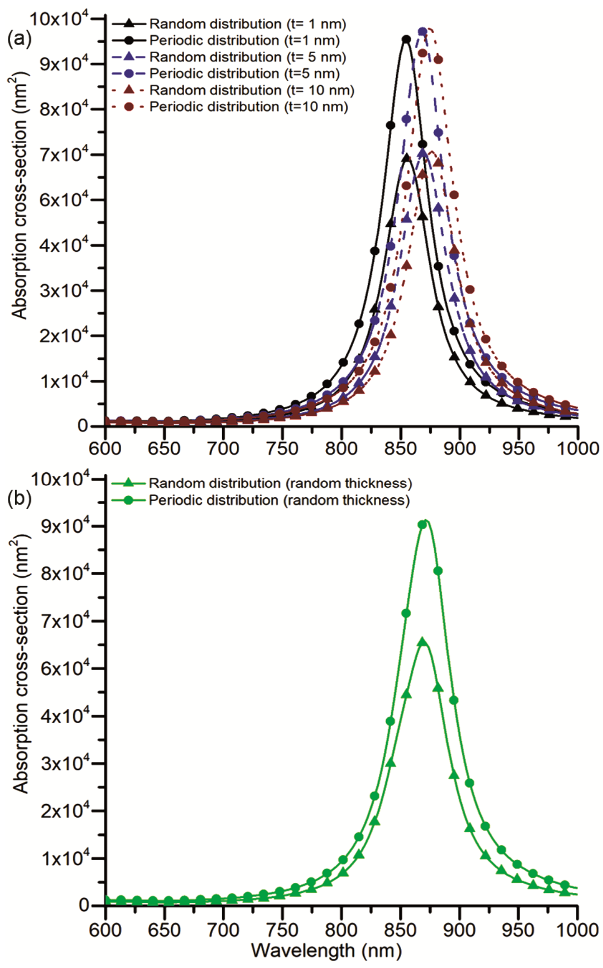

Fig. 6 — Spectral variation in σ_{abs} of breast tumor embedded with GNRs@SiO_2 of concentration 200 µg/ml with periodic and random spatial distributions for (a) uniform silica coating thickness (t) = 1 nm, 5 nm, 10 nm, and (b) random silica coating thickness within 1-20 nm.

distribution is ~44% higher as compared to random distribution for silica coating thicknesses of 1 nm, 5 nm, and 10 nm.

The spectral variation in σ_{abs} of breast tumor embedded with GNRs@SiO_2 of 1-20 nm random thicknesses and random spatial distribution is shown in Fig. 6(b). From Fig. 6(b), it is seen that the media embedded with periodically distributed GNRs@SiO_2 attained ~44% higher peak absorption cross-section as compared to randomly distributed nanoparticles. Additionally, despite the random and periodic spatial distribution of GNRs@SiO_2, there is no discernible change in plasmonic wavelength was observed. This result shows that the σ_{abs} of the media is highly affected by the orientation of nanoparticles w.r.t. the incident beam.

4 Conclusions

The computed results show that on increasing the silica thickness from 1 nm to 20 nm, significant changes in the optical properties of breast tumor media are observed. The absorption cross-section of breast tumors embedded with GNRs@SiO_2 of concentration 20 µg/ml with silica thickness 1 nm is increased by ~4.5%, while the scattering cross-section increases by ~8% as compared to media embedded with bare GNRs. On increasing the silica coating thickness by 1-20 nm on GNR, the scattering cross-section of media is significantly increased by ~26%, while a minor increase in absorption cross-section is observed. Furthermore, the plasmonic wavelength is shifted by 24 nm on increasing the silica thickness from 1-20 nm. The electric field is prominent up to the surface of silica coating, when silica thickness is>5 nm, while for silica thickness up to 5 nm, the field is confined within the core of silica coating. Computations considering spatial distribution of GNRs@SiO_2 in the medium show that tumor medium embedded with periodically distributed GNRs@SiO_2 possess absorption cross-section ~44% higher as compared to the randomly distributed nanoparticles. These discussed results are useful for the selection of silica coating thickness on GNRs for biomedical applications such as plasmonic photothermal therapy and photothermal induced drug delivery.

Acknowledgment

Vikas and Rizul Gautam gratefully acknowledge the fellowship from the Indian Council of Medical Research, Delhi, India vide grant number 5/3/8/83/ITR-F/2020-ITR and 5/3/8/37/ITR-F/2020 respectively. The authors acknowledge CSIR-Central Scientific Instruments Organisation, Chandigarh, India, for providing the infrastructure support.

References

1 Mercadal P A, Perez L A & Coronado E A, *J Phys Chem C,* 125 (2021) 15516.
2 Gorelikov I & Matsuura N, *Nano lett*, 8 (2008) 369.
3 Gao Z, Burrows N D, Valley N A, Schatz G C, Murphy C J & Haynes C L, *Analyst*, 141 (2016) 5088.
4 Ha L N T, Phan A D, Van K B T, Thuy N T, Trong N N, My N H T, Hong N T, Quang H D, Duong V & Minh H N, *ACS Omega*, 5 (2020) 20231.
5 Liu J, Detrembleur C, De Pauw-Gillet M C, Mornet S, Jérôme C & Duguet E, *Small*, 11 (2015) 2323.
6 Hanske C, Sanz-Ortiz M N & Liz-Marzán L M, *Adv Mater*, 30 (2018) 1707003.
7 Kennedy L C, Bickford L R, Lewinski N A, Coughlin A J, Hu Y, Day E S, West J L & Drezek R A, *Small*, 7 (2011) 169.
8 Diallo A T, Tlemçani M, Khan M, Spadavecchia J & Djaker N, *Part Part Syst Charact,* 37 (2020) 2000255.
9 Moustaoui H, Saber J, Djeddi I, Liu Q, Diallo A T, Spadavecchia J, Lamy de la Chapelle M & Djaker N, *J Phys Chem C*, 123 (2019) 17548.
10 Soni S, Tyagi H, Taylor R A & Kumar A, *Int J Hyperth*, 29 (2013) 87.
11 Vikas, Kumar R & Soni S, *Plasmonics*, 17 (2022) 107.
12 Wu W C & Tracy J B, *Chem Mater*, 27 (2015) 2888.
13 Davletshin Y R, Lombardi A, Cardinal M F, Juvé V, Crut A, Maioli P, Liz-Marzan L M, Vallée F, Fatti N D & Kumaradas J C, *ACS Nano*, 6 (2012) 8183.
14 Johnson P B & Christy R W, *Phys Rev B*, 6 (1972) 4370.
15 Ash C, Dubec M, Donne K & Bashford T, *Lasers Med Sci* 32 (2017) 1909.
16 O'Neal D P, Hirsch L R, Halas N J, Payne J D & West J L, *Cancer Lett*, 209 (2004) 171.
17 Das B B, Liu F & Alfano R R, *Rep Prog Phys,* 60 (1997) 227.
18 Vikas, Kumar R & Soni S, *Appl Nanosci,* 11 (2021) 2589.
19 Chen Y S, Frey W, Kim S, Homan K, Kruizinga P, Sokolov K & Emelianov S, *Opt express*, 18 (2010) 8867.
20 Abadeer N S, Brennan M R, Wilson W L & Murphy C J, *ACS Nano*, 8 (2014) 8392.
21 Wu W C & Tracy J B, *Chem Mater*, 27 (2015) 2888.
22 Vikas, Kumar R & Soni S, *Beilstein J Nanotechnol*, 14 (2023) 205.
23 Alrahili M, Savchuk V, McNear K et al., *Sci Rep*, 10 (2020) 18790.